

N75 11299

A SYNOPTIC STUDY OF SUDDEN PHASE ANOMALIES (SPA's)  
EFFECTING VLF NAVIGATION AND TIMING

E. R. Swanson  
C. P. Kugel  
Naval Electronics Laboratory Center

ABSTRACT

Sudden phase anomalies (SPA's) observed on VLF recordings are related to Sudden Ionospheric Disturbances (SID's) due to solar flairs. This study presents SPA statistics on 500 events observed in New York during the ten year period 1961 to 1970. Signals were at 10.2kHz and 13.6 kHz emitted from the OMEGA transmitters in Hawaii and Trinidad. A relationship between SPA frequency and sun spot number was observed. For sun spot number near 85, about one SPA per day will be observed somewhere in the world. SPA activity nearly vanishes during periods of low sun spot number. During years of high solar activity, phase perturbations observed near noon are dominated by SPA effects beyond the 95th percentile. The SPA's can be represented by a rapid phase run-off which is approximately linear in time, peaking in about 6 minutes, and followed by a linear recovery. Typical duration is 49 minutes.

INTRODUCTION

Periodically, portions of the 'surface' of the sun near sunspots are known to erupt or 'flare', thereby giving off large bursts of various forms of radiation. Flares producing sufficient amounts of energy in the X-ray portion of the spectrum are known to be the cause of sudden changes in the ionization of the earth's daytime D-region. This type of Sudden Ionospheric Disturbance (SID) may be evidenced as a Sudden Phase Advance or Anomaly (SPA) as observed on recordings of Very Low Frequency (VLF) radio signals received over long paths. The typically observed phase variation as a function of time is shown in Figure 1, including short term variations due to atmospheric noise; an idealized triangular waveform used as a theoretical model for the assumed variation is detailed in Figure 2.

This paper presents the results of a synoptic study of SPA's observed over North America from 1961 to 1970 as recorded on VLF signals propagating from the Omega Navigation System transmitter in Hawaii to an Omega receiving site at Rome, New York. Results of a shorter-term study from 1966 through 1970 over the path from the Omega transmitter in Trinidad to Rome also are presented. Parameters investigated include those noted on Figure 2, onset and recovery

PRECEDING PAGE BLANK NOT FILMED

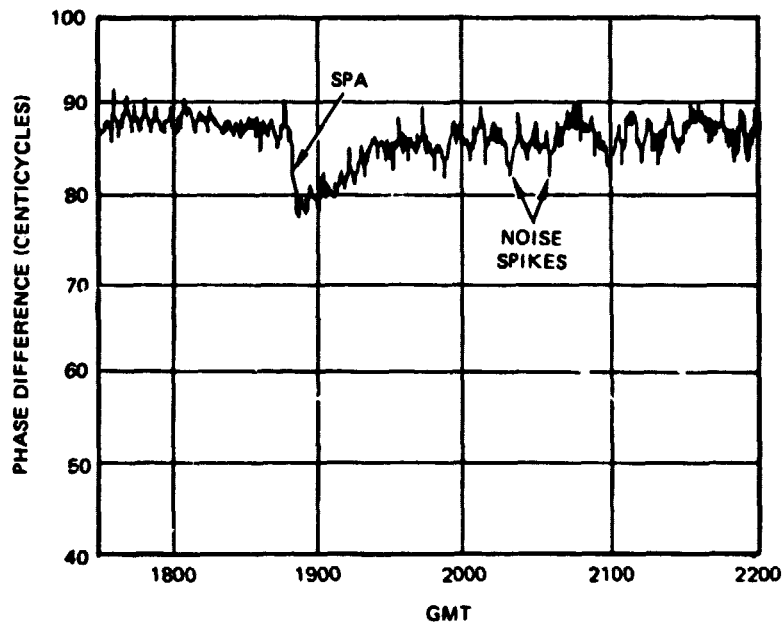


Figure 1. Typical VLF Phase Disturbance Caused by Solar X-ray Flare

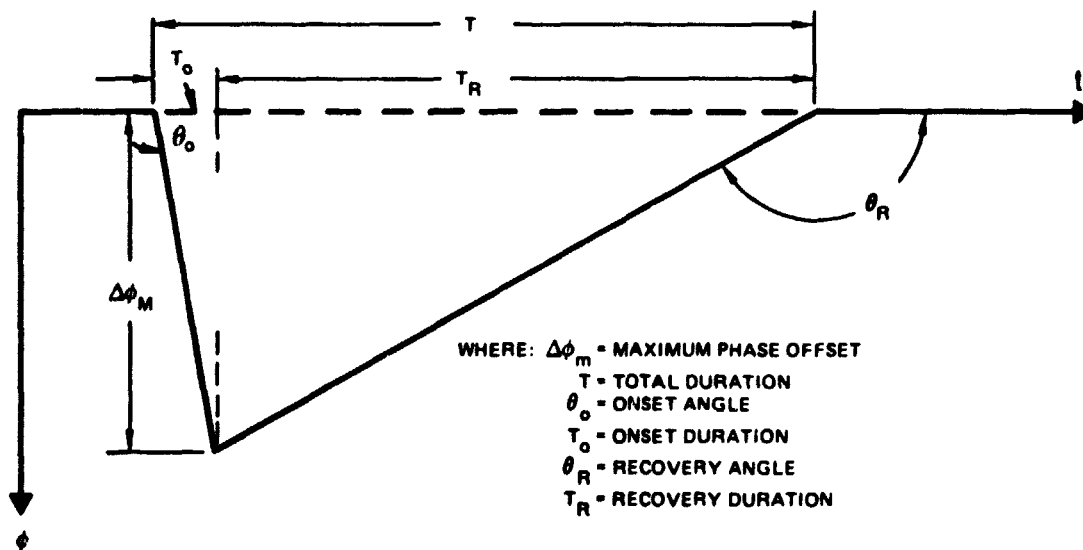


Figure 2. Idealized SPA Shape

rates, and cumulative disturbance probabilities. Distribution functions for the parameters were obtained together with interrelationships and behaviour with carrier frequency, sunspot number, solar zenith angle, and propagation path length.

An important feature of the present investigation is its restriction to synoptic data. No attempt has been made to relate results to particular geophysical morphologies or to direct data on observed solar X-ray flux. The approach taken was direct application to general error considerations for the Omega navigation system or other VLF navigation or communication system. For any particular specified application, especially one where the X-ray flux from the observed or anticipated flares can be determined, more complex analysis may be warranted. Additional information on the physics of solar flares especially their effects on solar flares can be found in References 1 through 4 of which Reference 4 includes an especially thorough study of one particular SPA for which the associated flux data was known. References 5, 6 and 7 provide additional information on the Omega system.

- a. Propagation path length
- b. Solar zenith angle on path
- c. Sunspot number

4. 'Probability' curves giving the percentage of time that propagation was disturbed above a certain level.

Due to the scarcity of Omega data and the low level of solar activity during the early 1960's, most of the foregoing results are derived from 10.2 kHz signals over the Hawaii to New York path from 1966 to 1970. In general, all results in this paper are intended only as summaries of observed effects of SPA's on Omega signals and have not been related to possible physical or chemical aspects of flare effects. Additional information on the physics of solar flares<sup>1,2,3,4</sup>, as well as the Omega System<sup>5,6,7</sup>, is available in the literature.

#### DATA AND COMPILATION PROCEDURES

The major source of data for this study was the Omega VLF phase difference measurements at 10.2 and 13.6 kHz recorded on strip charts at the Rome Air Development Center (RADC),<sup>8</sup> New York through 1970. The data represent the observed phase difference between the long-path signals from Hawaii (7814 km) or Trinidad (3843 km) and the groundwave signal from the local Omega transmitter at Forestport, New York (36 km).

As the signals from all Omega transmitters were being maintained by synchronism either by a master-slave mode of operation or by cesium-standard clocks,<sup>9</sup> these recordings indicate the absolute effect of ionospheric variation on the behavior of the long propagation paths. Data were available essentially continuously from January 1966 and partially from 1961 on 10.2 kHz.

Statistical data were obtained by manually scanning the recorded charts for SPA's and measuring observed times, rates and offsets. The time and phase offset determinations were straightforward; rates were indirectly determined by assuming the triangular shape of Figure 2 and obtaining the slope of the onset and recovery 'legs' of the triangle. The onset slope normally followed the recorded rapid shift exactly; the recovery slope was determined from an eyeball 'best-fit' line tangent to the half-magnitude point of the recovery period. Deviations from the assumed triangular shape were also tabulated for the larger events. Although all detectable events were noted, shape characteristics were compiled only for those events falling within a 'day window' centered about mid-path noon. This window varied seasonally from 4 hours in winter to 8 hours in summer and was typically about 2040 hours per year. This restriction was imposed to prevent the curvature in the diurnal phase variation during sunrise and sunset transitions from affecting the apparent phase rates-of-change and offsets caused by SPA's. Two other restrictions on the compilation of events involved very small (5 cec or less) and multiple SPA's. Disturbances of 5 cec\* or less have been excluded from all analyses due to both the difficulty in detecting such events in the normal propagation noise and to the desire to limit the number of events to those exhibiting a shape sufficient for analysis on the scale of the phase recording charts. A 5 cec SPA amounts to less than 0.25 inch on the typical track of an Omega recording, so detection and/or analysis of smaller events was considered impractical.

Multiple SPA's; i. e., additional disturbances occurring before the initial event was recovered completely, were included in only those analyses for which the relevant shape characteristics could be determined reliably. As an example, these events were included in the probability of disturbance and cumulative analyses but not in any of the shape correlation analyses. The possible effects of inclusion or exclusion of multiple SPA's, as well as the other constraints, are discussed wherever applicable in the "results" sections to follow.

Before presenting any results however, the possible effects of equipment and the applicability of various types of units will be discussed.

---

\*1 cec = 1 centicycle = 0.01 cycle. See following sections.

## EQUIPMENT

In general, the receiving equipment at the Omega system monitoring sites was designed either for use in controlling the timing synchronization of the associated transmitters or for general navigation aboard relatively slow-moving vehicles. The receiver time constants (approximately 30-60 seconds) and tracking rates were, therefore, selected to adequately perform these system-oriented tasks with only secondary priority attached to the accurate representation of propagation anomalies. Abrupt phase changes were not expected during normal operation so that some smoothing over several 10-second transmission format intervals was not only acceptable but also desirable for noise-reduction purposes. None-the-less, the typical time constant was about one minute and the equipment was capable of slewing up to 10 cec per min, which the following discussion will show to be adequate for this study.

The distortion to input phase variations caused by the receiver can be assessed easily by considering two special cases; an abrupt received phase disturbance and a ramping one. In the case of an abrupt input phase shift greater than 10 centicycles (cec), the output would ramp at the maximum slew rate of 10 cec/min. In practice, a typical magnitude was 15 cec and the typical onset rate was 3.5 cec/minute so that the observed onset rate must be indicative of primarily the actual input phase rate. In the case of a ramped input phase variation, the observed steady state output will also ramp but delayed from the input by the one-minute time constant; within the first minute or so, there will be a slight non-linearity between the steady-state ramping and the actual onset. Presumably, this slight non-linearity will be difficult to detect due to normal noise effects on the phase recordings and the principal effect will be to delay the apparent onset time by about one minute rather than affect the observed duration or time to maximum onset. Thus the receiving instrumentation is not believed to have had a significant effect on the important statistics considered.

Some scatter must reflect inability to precisely scale the recorded data. All but a few months of data were recorded on linear chart paper having a phase scale of 1 cycle full-scale equal to 4.5" and a take-up rate of 3"/hr before 1966 to 3/4"/hr after 1965. The remaining data were recorded on curvilinear paper with a 4.5"/cycle phase scale and a 3/4"/hr take-up rate. The precision of the recorded phase and time readings were about 1 centicycle (cec) and 2 or 3 minutes at the slowest chart speed, respectively. The precision of the slope measurements was about 1 degree. As the typical observed onset slope of SPA's was about 85° (approx. 3 cec/min), the rapid change in the tangent in this region will cause the rate uncertainty to increase directly with rate and become approximately 7 cec/min for 89°. Since the maximum receiver tracking rate of 10 cec/min corresponds to angle of 88.5°, the few observed rates in this region and the high associated uncertainty lead to the conclusion that the equipment was not a factor

in limiting the recorded shape behavior of the SPA's. The two events in 1969 with angles of  $89^\circ$  supposedly are not possible, due to equipment limitations, but are most probably due to the measurement uncertainty.

#### PHASE ANOMALY SIGNIFICANCE AND UNITS

All primary statistics in this paper are expressed in units of the experimentally observed phase changes or rates over the propagation path being investigated. While lacking universality, the approach renders the statistics independent of assumed ionospheric models. To assist in making the results more meaningful, additional scales have been superimposed in which the observed variations are associated with "equivalent" changes.

Experimental measurements were made in angular units of centicycles (1 centicycle = 1 cec = 0.01 cycle). It is often common practice to draw an "equivalence" between phase and time by associating one cycle of the carrier with one period.<sup>10, 11</sup> At 10.2 kHz this yields 1 cec  $\sim 1 \mu s$  while at 13.6 kHz, 1 cec  $\sim 3/4 \mu s$ . A similar relation between phase and "equivalent" distance when ranging may be obtained by associating one cycle with one wavelength. The wave length at 10.2 kHz is 30 km so that 1 cec  $\sim 0.3$  km distance while at 13.6 kHz, 1 cec  $\sim 0.23$  km distance. (In the hyperbolic phase difference mode usually used with Omega, these distance equivalences are approximately halved so that 1 cec  $\sim 0.15$  km.) Associated rates follow directly: one centicycle/minute corresponds to a fractional frequency variation of  $1.7 \times 10^{-8}$  at 10.2 kHz and  $1.3 \times 10^{-8}$  at 13.6 kHz. Velocity equivalences when interpreted for radial ranging are 1 centicycle/minute  $\sim 18$  km/hr at 10.2 kHz or 14 km/hr at 13.6 kHz. Another association which is often made is that between phase variation and ionospheric height change. In the common calculation, the path length is divided by the time equivalent phase variation to obtain a velocity variation. The velocity variation is associated with an equivalent change in the height of the earth-ionosphere waveguide necessary to match the computed velocity variation. The difficulty with this method is that it assumes the phase shift is entirely due to an effective height change rather than changes in ionospheric electron density gradient or other process. Further, the calculation is valid only if the excitation factor remains constant. An additional complication, discussed in a subsequent section, is whether the calculation should use the entire propagation path length. Despite the limitations, "equivalent" height variations<sup>7</sup> have been associated with the data based on a partial relative velocity variation with height of  $3.2 \times 10^{-4}$  /km at 10.2 kHz and  $1.9 \times 10^{-4}$  /km at 13.6 kHz corresponding to equivalent height changes of 0.12 and 0.15 km per centicycle at 10.2 and 13.6 kHz respectively over the Hawaii-New York path and twice as much over the Trinidad-New York path.

## RESULTS

### Maximum Phase Offset Distributions

Figure 3 gives the number distributions of the maximum phase offsets produced by SPA's observed at 10.2 kHz on the Hawaii-New York path from 1966 through 1970. The data was quantized in 5 cec intervals, and include all observed events greater than 5 cec. Multiple SPA's have been included by considering the apparent additional offset produced by the subsequent events as being individual events. This procedure has had the most significant effect in 1967 and 1970 wherein the number of observed events has been increased by 20-25%. For other years the effects were 10% or less, and no significant effect on the overall distributions was found.

Several features are apparent from Figure 3. There are fewer SPA's and they are smaller during periods of lower solar activity (1966-1967) than near solar cycle maximum (1968-1970). The phase change typically peaks between 10-15 cec corresponding to ionospheric phase-height changes of 1.2 to 1.8 km. For SPA's greater than 5 cec, the average magnitude was 23 cec corresponding to height changes of 2.8 km. It is notable that in most years, fewer SPA's were observed with amplitude between 5 and 10 cec than were observed with amplitude between 10 and 15 cec. The distribution thus does not appear of the type where there is a very large probability of small events such as might be expected if SPA's were but rare manifestations of a phenomenon characteristic to normal ionospheric formation. Instead, the distributions suggest SPA's and the causal solar flares are specific identifiable events which tend to have typical magnitudes characteristic of the flare formation physics.

### Onset Phase Rate-of-Change Distributions

The number distributions for the onset rate-of-phase-change for various years are shown in Figure 4. The distributions appear similar and essentially normal in each year differing primarily in the fewer events observed during lower solar activity in 1966. The median onset rate is 3.5 cec/minute which corresponds to a fractional frequency shift of  $6 \times 10^{-8}$  equivalent to a radial-range rate of 63 km/hr. The associated rate of lowering of the ionospheric phase height is about 0.4 kilometer per minute.

The observed onset rates are generally well within instrumental capabilities and thus are believed to indicate true ionospheric changes. The two extreme rates in 1969 may be the result of measurement uncertainty whereas the near absence of rates between 4 and 5 and between 6 and 7 cec/min is due to roundoff of the onset angle during scaling.

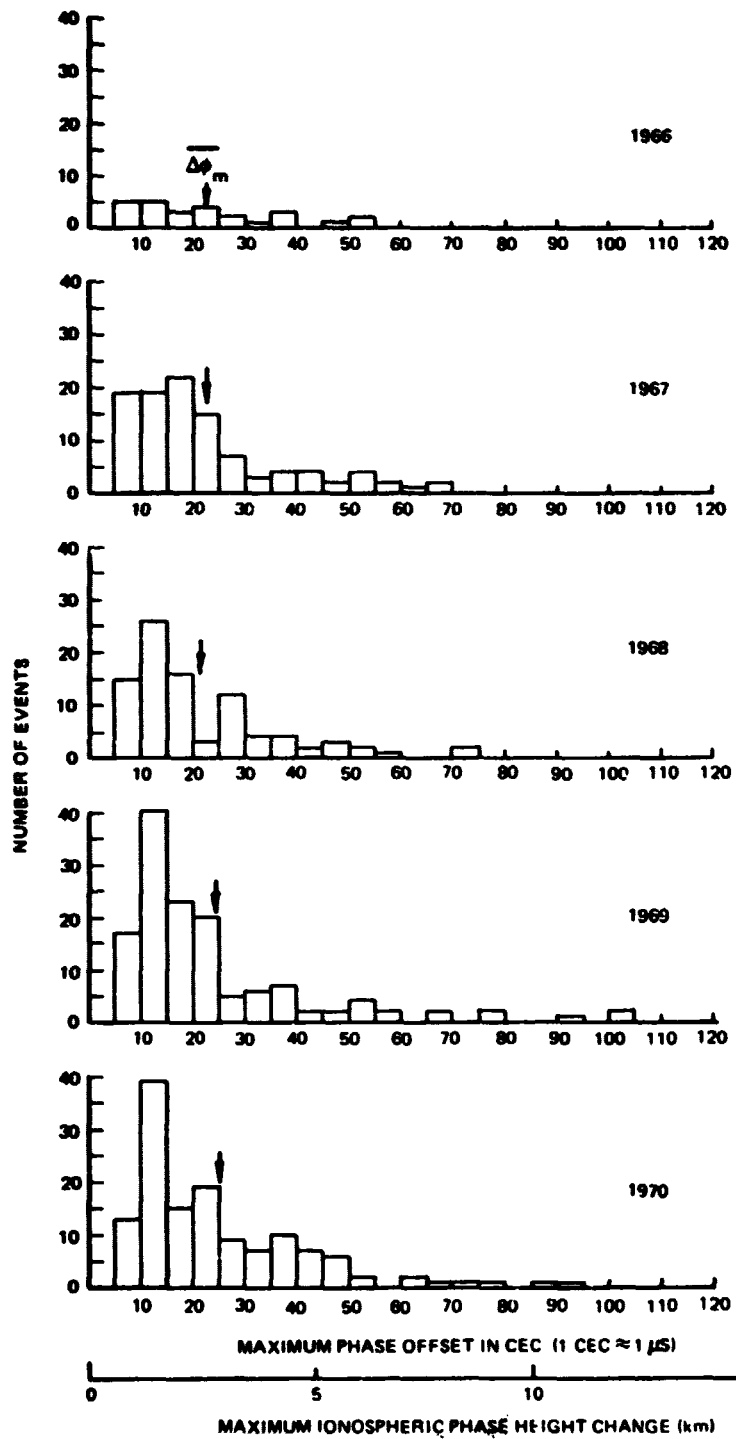


Figure 3. Maximum Phase-Offset Distributions Observed During SPA Events on Hawaii to New York Path at 10.2 kHz

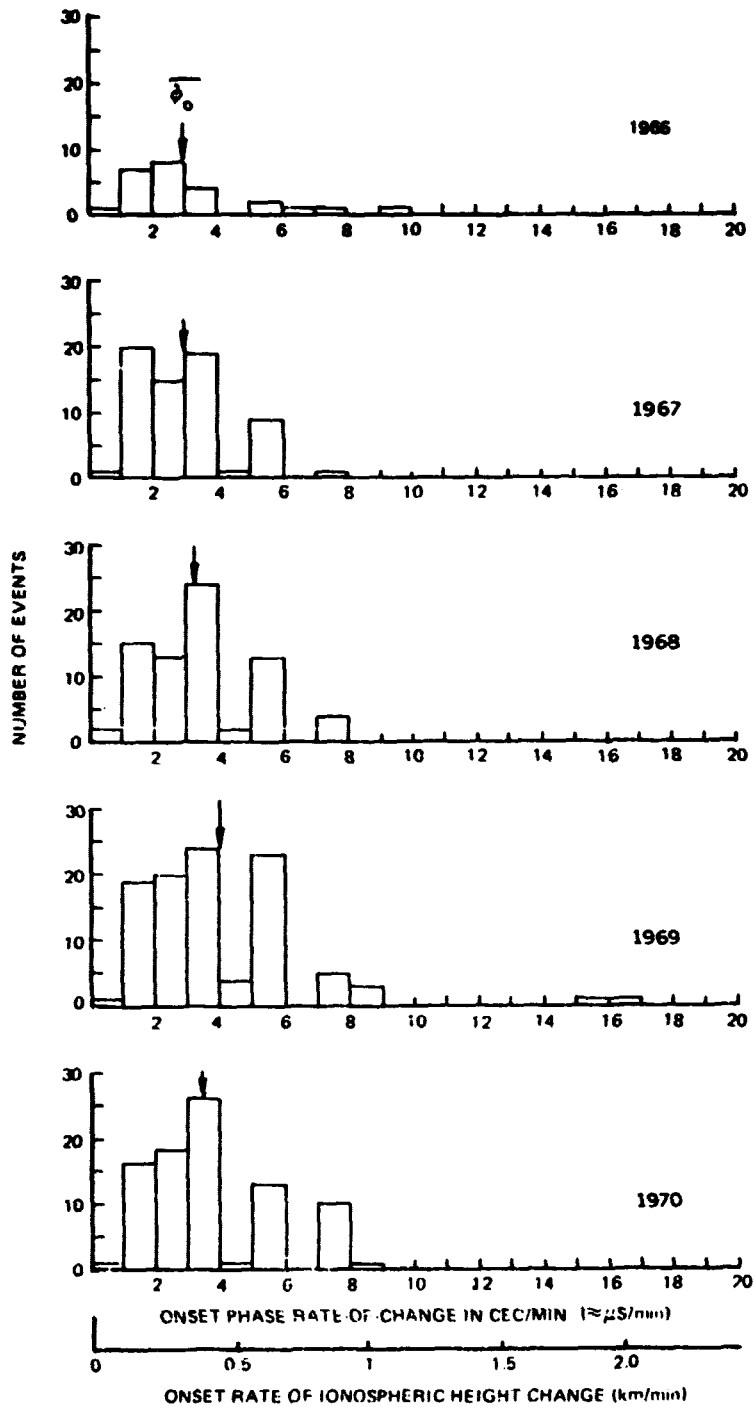


Figure 4. Onset Phase Rate-of-Change Distributions Observed During SPA Events on Hawaii to New York Path at 10.2 kHz

In this and the following 2 sections, multiple SPA's have been excluded because of the difficulty in determining the rates-of-change and duration of individual events in the disturbance.

#### Disturbance Duration Distributions

Figure 5 shows the number distributions for duration of SPA disturbances observed during the same data sample used to show amplitude distribution in the previous section. The plots indicate a peaking effect around 40 minutes or so with a decrease in frequency with length of disturbance. Except for the minor occurrence of a few longer SPA's in the latter years, there does not appear to be any significant variation of disturbance duration with sunspot number, which nearly tripled over the time span being analyzed.

As will be discussed in the following section on decay rates-of-change, the disturbance duration may have been significantly shortened by the modeling approximation used for the 'recovery' leg of the event. For a typical duration of 40 minutes, an error of 10% is significant but probably unimportant in a practical sense.

#### Recovery Phase Rate-of-Change Distributions

Figure 6 shows the number distribution for the decay rates-of-change of phase for the same data sample as previously shown. The peak occurrence is at 0.5 cec/min or less for each year and the distributions are not quite normal with the heaviest weighting occurring at the slower rates.

As noted in the data section, the decay rate was determined from an approximate linear fit to the normally exponential recovery exhibited by the typical SPA. An investigation of the possible errors introduced by this approximation indicated that the decay slope estimation usually was biased toward the early portion of the recovery period and therefore resulted in a higher indicated overall decay rate, and subsequently, a shorter indicated duration of the disturbance. This systematic error will not significantly affect the decay rate statistics, as long as they are understood to apply to all but the final portion of the recovery period. However, the duration statistics may be significantly affected as was discussed previously.

#### Disturbance Level Probability Analysis

A most useful statistic describing the effects of SPA's is the percentage of time that an Omega Phase track is likely to be disturbed above a given value. Such information may be extracted from historical data summarized according to time span and the percentage of time the observed disturbances exceeded various incremental levels. Assuming that the chronological variation of SPA occurrence

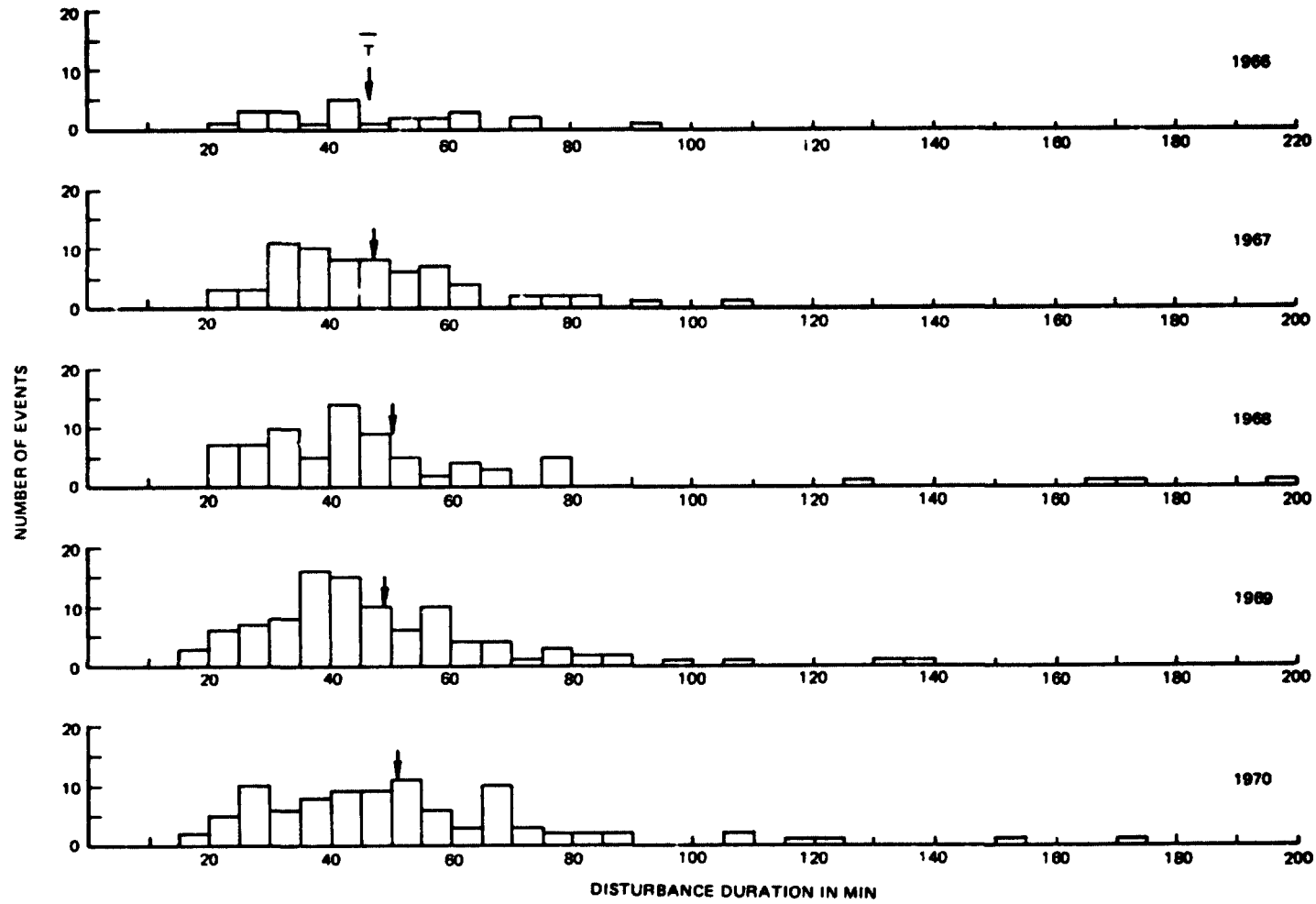


Figure 5. Disturbance Duration Distributions Observed During SPA Events on Hawaii to New York Path at 10.2 kHz

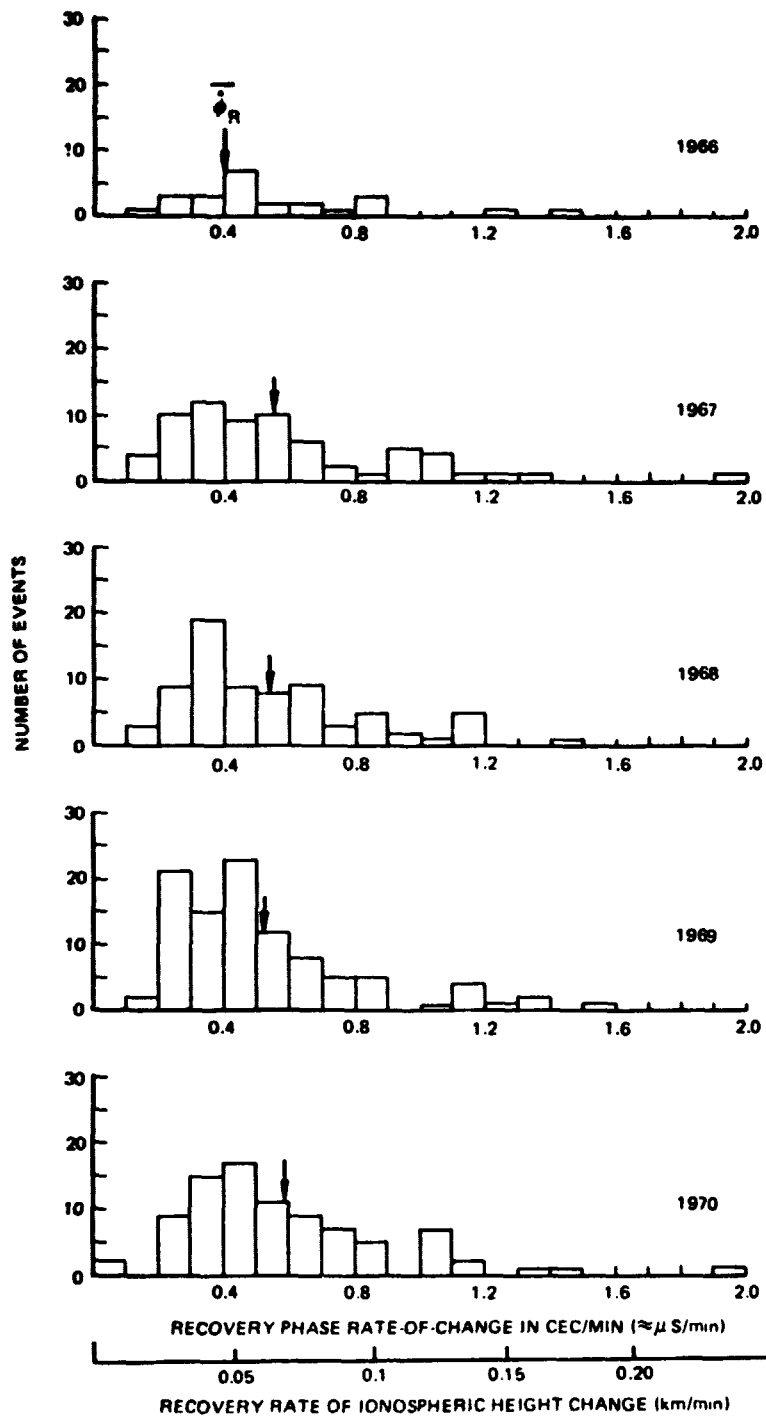


Figure 6. Recovery Phase Rate-of-Change Distributions Observed During SPA Events on Hawaii to New York Path at 10.2 kHz

can be related to some solar activity indicator (e.g., sunspot number), the historical statistics may be interpreted as the probability of occurrence of disturbances during any given period of solar activity.

The historical summaries may be obtained from the data compiled for this report by assuming SPA's to have the triangular shape of Figure 1 and a reference level  $\Delta\phi_c$  as shown in Figure 7. The total duration  $T$  of the SPA is computed from the tabulated maximum amplitude  $\Delta\phi_m$  and the onset and recovery angles  $\theta_o$  and  $\theta_R$ :

$$T = T_o + T_R = \frac{\Delta\phi_m}{\tan \theta_o} + \frac{\Delta\phi_m}{\tan (180 - \theta_R)} = \Delta\phi_m \left( \frac{1}{\tan \theta_o} + \frac{1}{|\tan \theta_R|} \right) \quad (1)$$

$$T = \Delta\phi_m \left( \frac{\tan \theta_o + |\tan \theta_R|}{\tan \theta_o |\tan \theta_R|} \right)$$

Using similar triangles, the duration  $T_c$  for which  $\Delta\phi$  exceeds the reference level  $\Delta\phi_c$  can be found from:

$$\frac{\Delta\phi_m}{T} = \frac{\Delta\phi_m - \Delta\phi_c}{T_c} \quad (2)$$

$$T_c = T \left( \frac{\Delta\phi_m - \Delta\phi_c}{\Delta\phi_m} \right) = T \left( 1 - \frac{\Delta\phi_c}{\Delta\phi_m} \right)$$

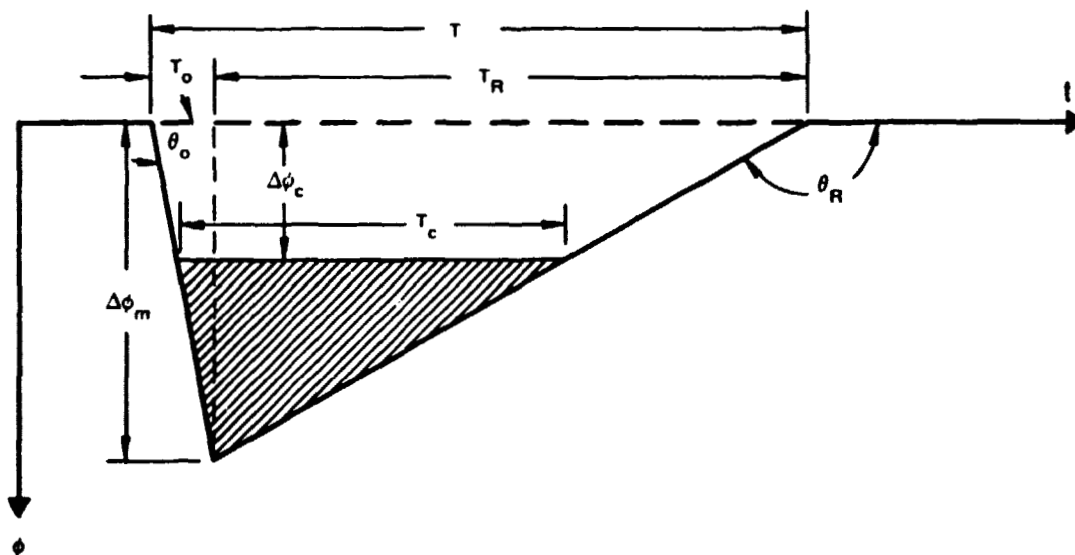


Figure 7. Idealized SPA Shape With Reference Level

As written, Equation 2 utilizes the amplitudes and rates of change obtained from the disturbances observed over a specific path under specific solar illumination conditions. When Equation 2 is divided by the total time available  $\Sigma T_0$  for detecting SPA's, the result is the percentage of time that the observed disturbances exceeded the specified reference level:

$$T_c(\%) = \frac{\Sigma T_i \left( 1 - \frac{\Delta\phi_c}{\Delta\phi_{m_i}} \right)}{\Sigma T_0} \quad (3)$$

If  $T_c(\%)$  is thought of as a percentage probability of occurrence, the notation can be changed to read:

$$P(\Delta\phi > \Delta\phi_c) = 100 T_c(\%) = 100 \frac{\Sigma T_i}{\Sigma T_0} \left( 1 - \frac{\Delta\phi_c}{\Delta\phi_{m_i}} \right) \quad (4)$$

Figure 8 gives plots of P for the years 1966 through 1970 over the range of applicable reference levels. The relative position of the curves tends to follow the variation of solar activity over this period, except for 1967, which appears more active than expected. This may have resulted from the procedure used to normalize the observed disturbed time to the total time available for observation. This normalization assumes a random distribution of SPA activity throughout the year and neglects any compression of activity into specific months or even weeks, which is typical of recent solar activity levels. As 1967 had significantly less observed time than other years, any error introduced by the normalization would be greater for that year. In addition, 1967 contained a greater number of multiple SPA's, which amounted to a significant proportion of the already very small percentage of disturbed time. After consideration for the high sensitivity of the computation in the region of low percentages, the overall result is in good agreement with that expected from the sunspot number variation during this period. The following section discusses the correlation of SPA activity and the yearly average sunspot number.

#### Frequency of SPA Occurrence with Sunspot Number

Figure 9 shows the observed variation of SPA occurrence with the National American sunspot number,  $R_A^{12}$ . The plotted data points have been determined from measurements at 10.2 kHz on the Hawaii to New York path and include all events greater than 5 cec as observed in a typically 6-hour duration 'window' near mid-path noon. The points shown for  $N_{24}$  are an extrapolation to the event levels expected under the condition of continuous solar influence over 24 hours. The curve for  $N_{12}$  is a similar extrapolation to a typical 'daylight' condition of 12 hours somewhere on the globe.

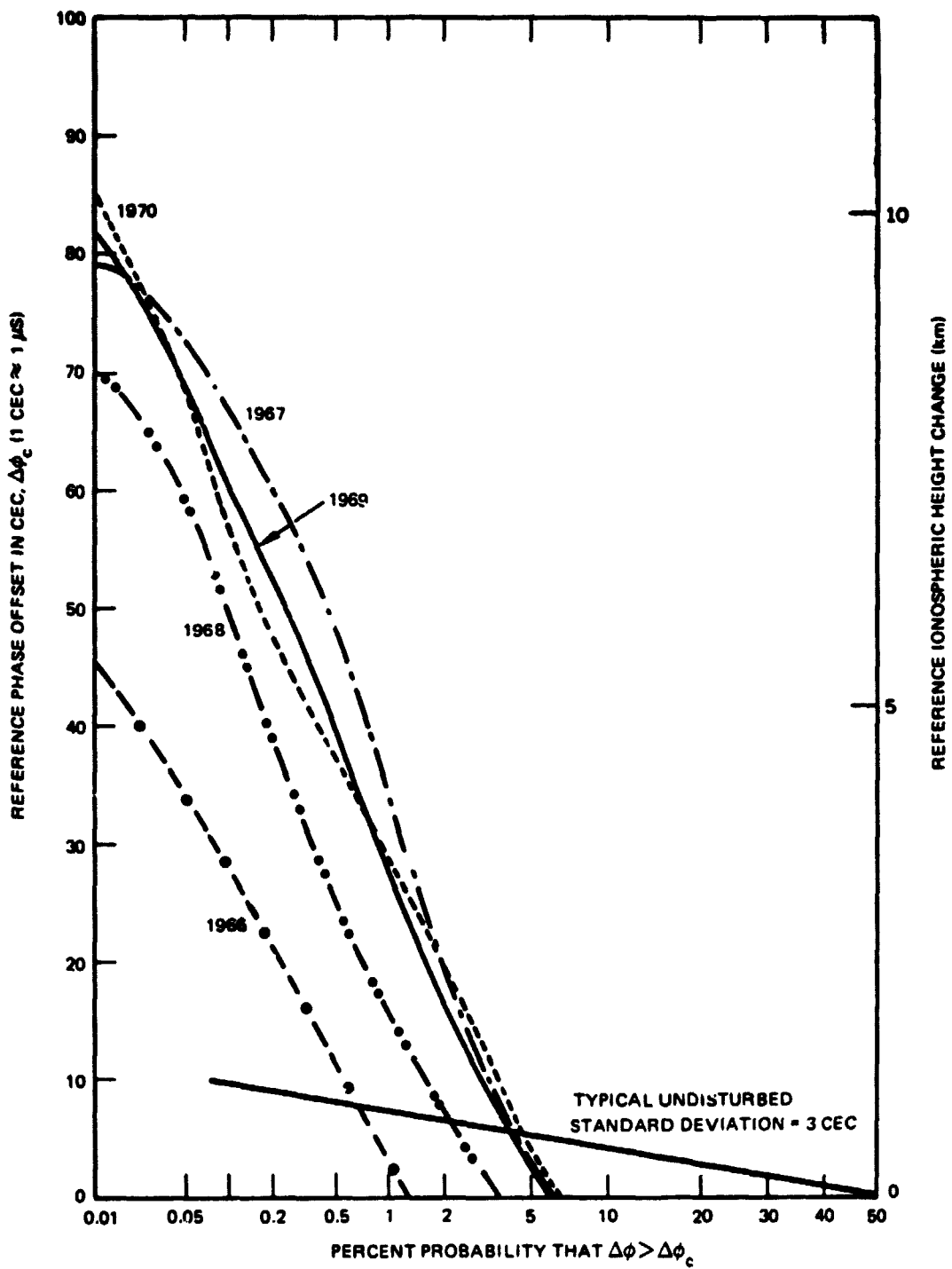


Figure 8. Percent Probability of Disturbance Level Occurrence for Observed SPA Events on Hawaii to New York Path at 10.2 kHz

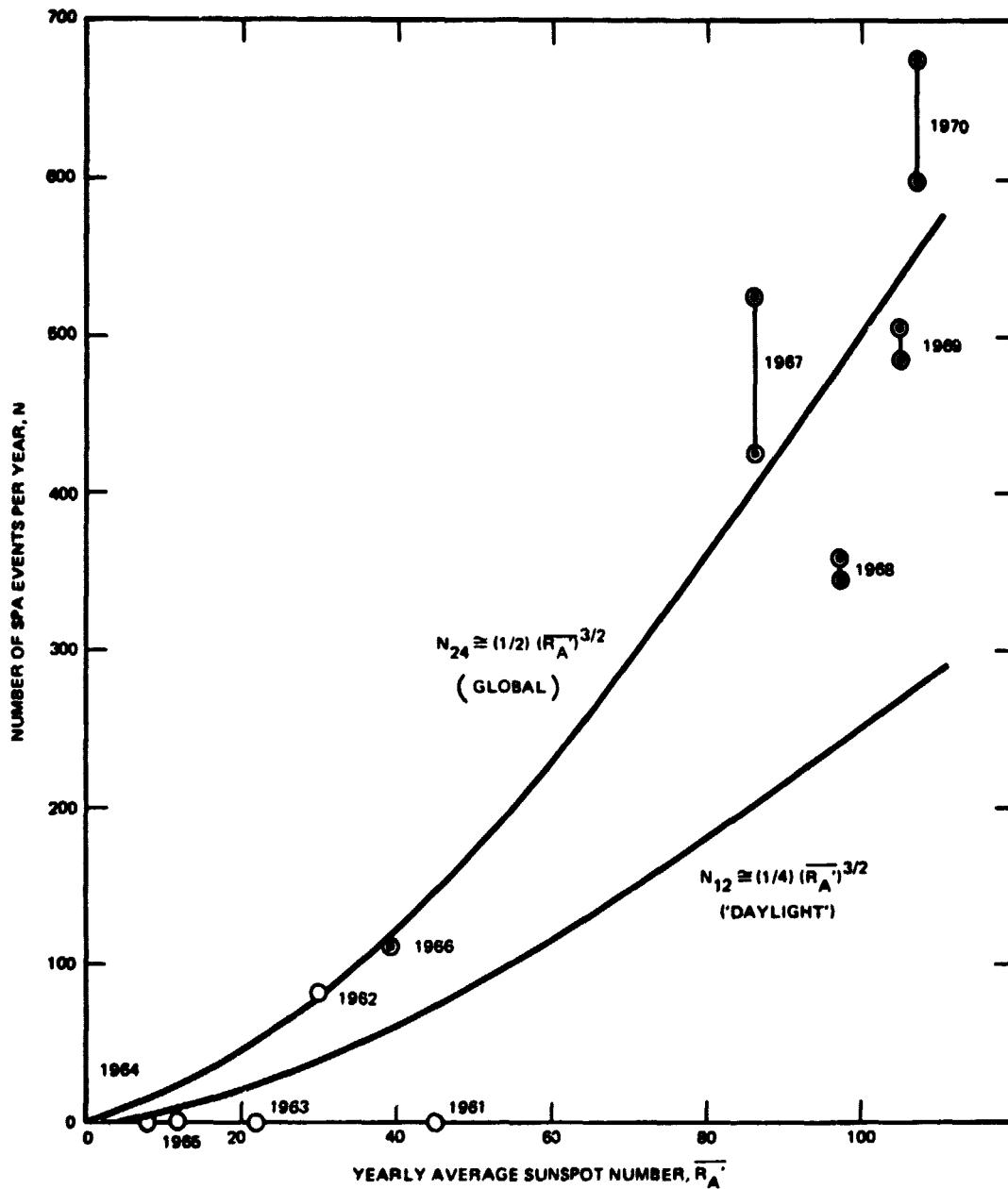


Figure 9. Variation of SPA Occurrence With Sunspot Number

The effect of multiple SPA's is shown by the double values plotted for certain years. The upper point includes all events discernible within the duration of the multiple disturbances; the lower point assumes each multiple event to be only a single disturbance. The largest effect is in 1967 which exhibited about 20% less observation time but proportionally more multiple events than other years.

The distribution functions of Figure 3 suggest that perhaps the event levels might be about 10% higher, if small comparatively unimportant events of less than 5 cec also had been included.

The empirical functions drawn on Figure 9 are simple approximations to the regression curve determined for the midpoints of the indicated range of events for the years 1966 through 1970. The midpoints were used as a compromise between the possible ways of counting multiple events. Data from 1961-1965, shown as open circles, were excluded from the fitting analysis because of the brief transmission schedule relative to the latter years and also the complexity in detecting the occurrence of events. For all years, the data were obtained by normalizing the observed number of events by the ratio of the total hours of recordings actually searched (500-2000 per year) to the number of hours available for observation (approx. 8800 and 4300 for the 24 and 12-hour functions).

The data indicate that a 'yearly average' sunspot number near 85 the frequency of occurrence of SPA's over the entire globe is statistically about one per day. There is also the suggestion of a non-linear relationship between SPA occurrence and sunspot activity with the occurrence nearly vanishing during years of low sunspots.

During 1961 there were 500 hours of transmission near noon while there were 750 hrs in 1962, 700 in 1963, 600 hrs in 1964 and 1000 hrs in 1965. Thus 1961-1965 probabilities are less statistically certain than those based on the nearly continuous transmissions schedule maintained in latter years. This is especially true for 1961 when there were no hours of simultaneous monitoring at both ends of the path. It was also more difficult to measure SPA's during 1961-1965 since the Omega system was not operated in the modern "absolute" configuration where each station operates directly from cesium standards but rather in the older system configuration wherein some stations were operated as "masters" and others as "slaves", which functioned to approximate in-phase reflectors of the master signals delayed by retransmission location in the 10-second time-sharing commutation pattern. During much of the early period a station in the Panama Canal Zone was operating as master with both Hawaii and New York operating as slaves. SPA's for the Hawaii to New York path were derived from measurements of the New York - Canal Zone master-slave pair near Hawaii and of the Hawaii - Canal Zone pair near New York. Propagationally, the former measurement includes transmission from the Canal Zone to Hawaii (CH) thence from Hawaii to New York (HN) measured with respect to transmission from the Canal Zone to New York (CN): Measurement #1 represents  $CH + HN - CN$ . Similarly, Measurement #2 represents  $CN + NH - CH$ . Thus the sum of the two measurement represents  $HN + NH$ , i.e., roundtrip propagation between Hawaii and New York. Since checks during other transmission periods indicate SPA's are similar in either propagation direction, the derived roundtrip is thus representative of the

Hawaii - New York measurement obtained directly in later years. Measurement of the multiple records is, however, awkward and subject to higher uncertainty than the direct measurement.

#### Variation of SPA Magnitude with VLF Frequency

The frequency dependence of SPA magnitudes is of interest both to the study of ionospheric behavior and for navigation using the Omega System. This behavior was investigated at the carrier frequencies of 10.2 and 13.6 kHz for both the Hawaii to New York and Trinidad to New York paths. Data were compiled for approximately 50 SPA's in each of the years 1967, 1969 and 1970 for the HA-NY path and a total of 50 SPA's for the years 1967 and 1970 on the TD-NY path. The events used were selected randomly from the total set and were determined mainly by their availability as individual events at both carrier frequencies.

Preliminary checks indicated that onset times and general shapes were the same for both frequencies for both paths being considered. The maximum phase off-sets then were used to determine the average and best-fit linear estimate of the slope of the  $\Delta\phi_{13.6}$  versus  $\Delta\phi_{10.2}$  function, with the comparisons being given in Figure 10 and summarized in Table I. The results indicate to a high degree of confidence that the relative SPA magnitude effects at 13.6 and 10.2 kHz are directly proportional, with the indicated proportionality constant of 0.75 being equal to the ratio of the carrier frequency wavelengths:

$$\Delta\phi_{13.6} = 0.75 \Delta\phi_{10.2} = \left( \frac{\lambda_{13.6}}{\lambda_{10.2}} \right) \Delta\phi_{10.2} \text{ (Cycles)}$$

which is as expected if the phase height variations estimated from data at either frequency are to be the same. Since no data at other frequencies were used, the applicability of the wavelength-ratio proportionality to other frequencies is unknown.

#### Correlation of SPA Shape Characteristics

Figures 11 through 13 show the functional interdependence of the various shape characteristics of the SPA's being studied. The plots are presented in a format intended to represent both the predictive as well as physical aspects of these relationships; i. e., how well one can predict the maximum phase offset from the observed run-off rate, or the disturbance duration or decay rate from the observed maximum offset. These relationships have been approximated by best-fit (least-squares) lines through the origin and with arbitrary intercept. The resulting slopes and correlations are tabulated in Table II; ordinate intercepts are shown on the figures. The 'true' best-fit line was computed to show both the correct sample correlation,  $r_B$ , and the discrepancy with the line through the origin.

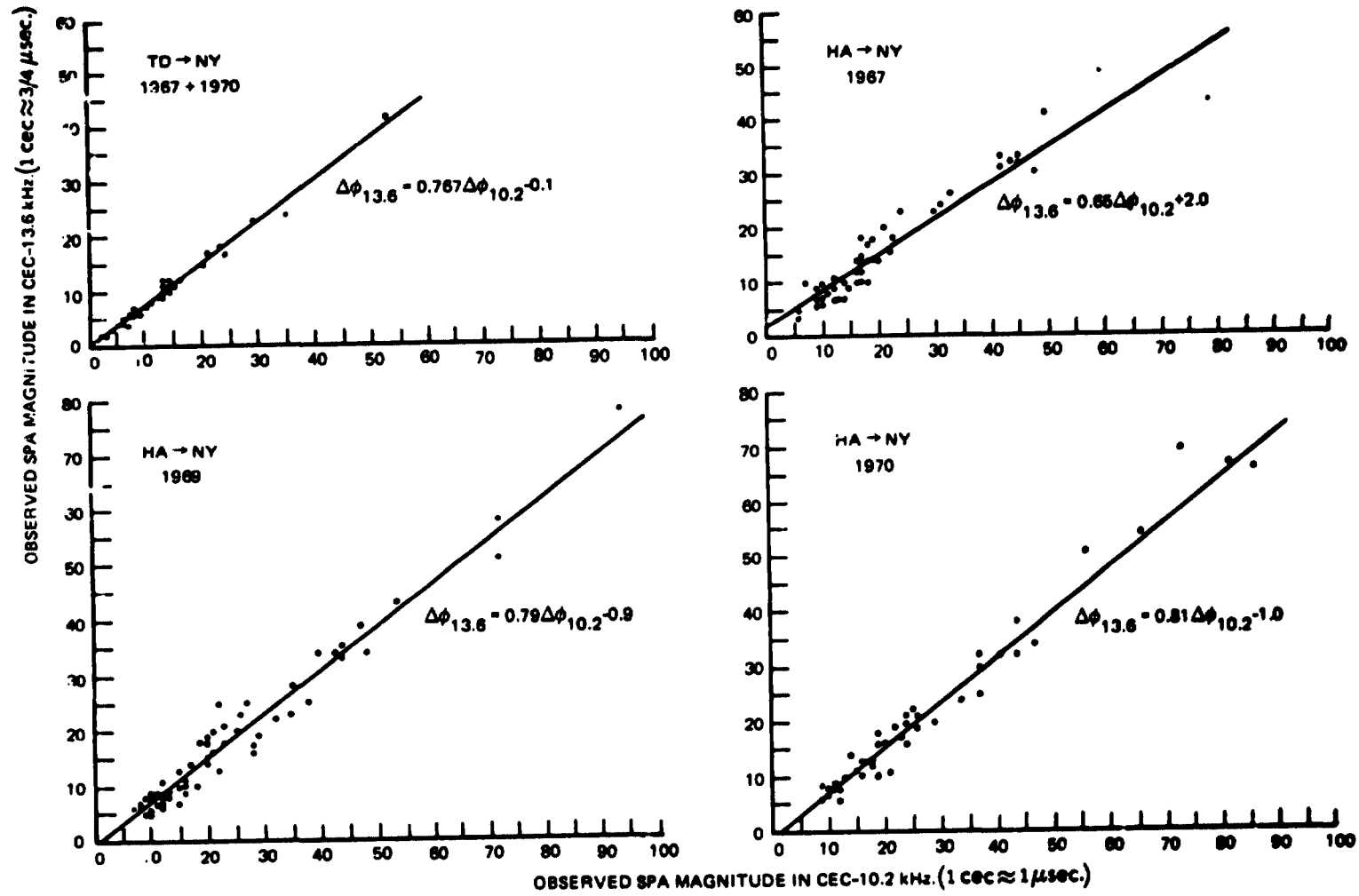


Figure 10. Frequency Correlation of Maximum Phase Offsets for SPA Events Observed Simultaneously on 10.2 and 13.6 kHz

Table I

Summary of SPA Magnitude Variation at 10.2 and 13.6 kHz

PATH	YEAR	SAMPLE SIZE	$\Delta\phi_{10.2}$ AVERAGE	$\Delta\phi_{13.6}$ AVERAGE	SLOPE AVERAGE	SLOPE LINEAR FIT	INTER- CEPT	SAMPLE CORRE- LATION
TD → NY	1967	47	11.8	9.0	0.763	0.77	-0.1	0.99
	1970							
HA → NY	1967	48	20.0	14.9	0.745	0.65	2.0	0.96
	1969	59	22.5	17.1	0.750	0.79	-0.9	0.98
	1970	41	26.3	20.4	0.775	0.81	-1.0	0.99
AVERAGES					0.758	0.75	0.0	0.98

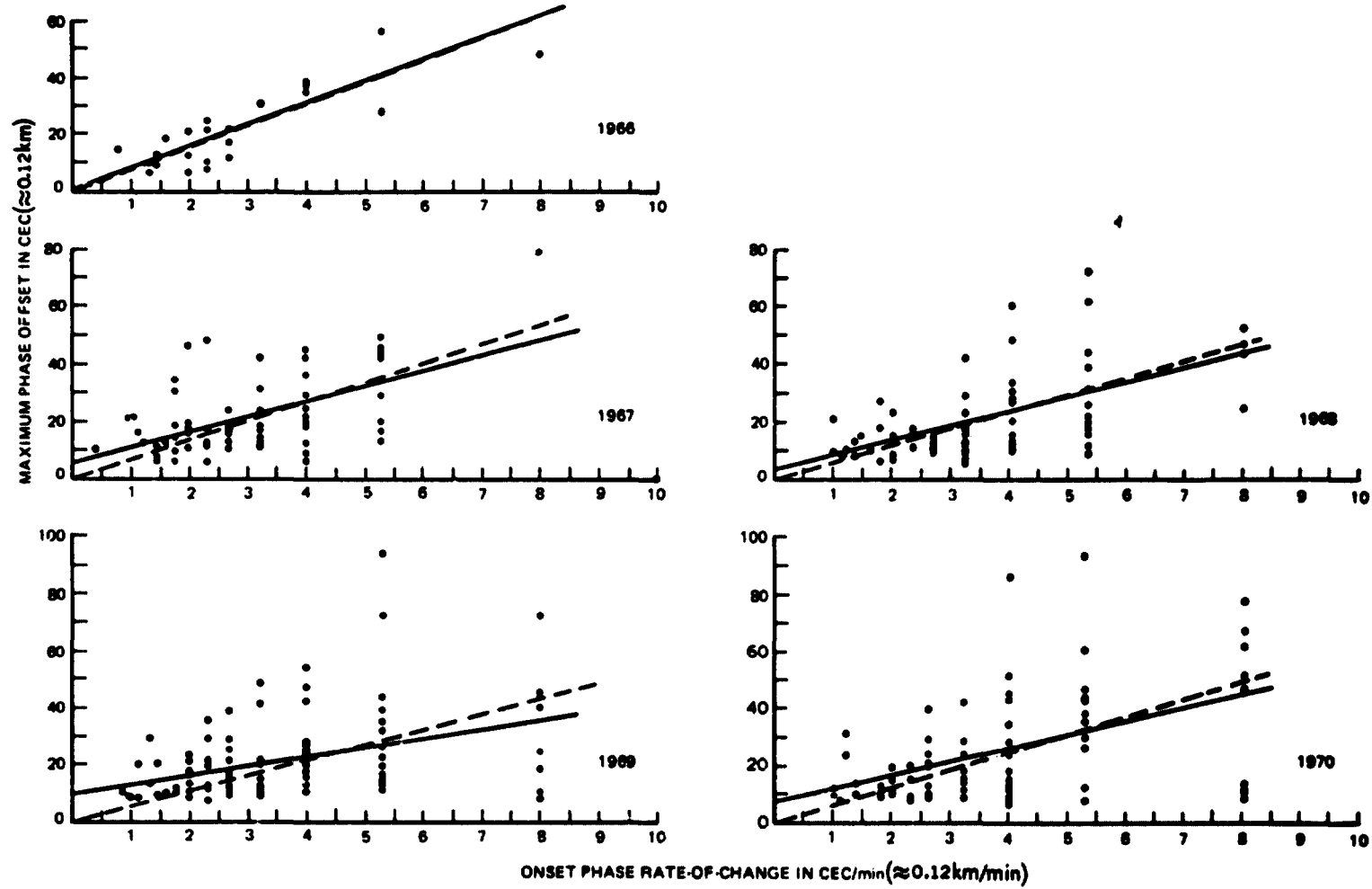


Figure 11. Maximum Phase Offset vs. Onset Phase Rate-of-Change for SPA Events on Hawaii to New York Path at 10.2 kHz

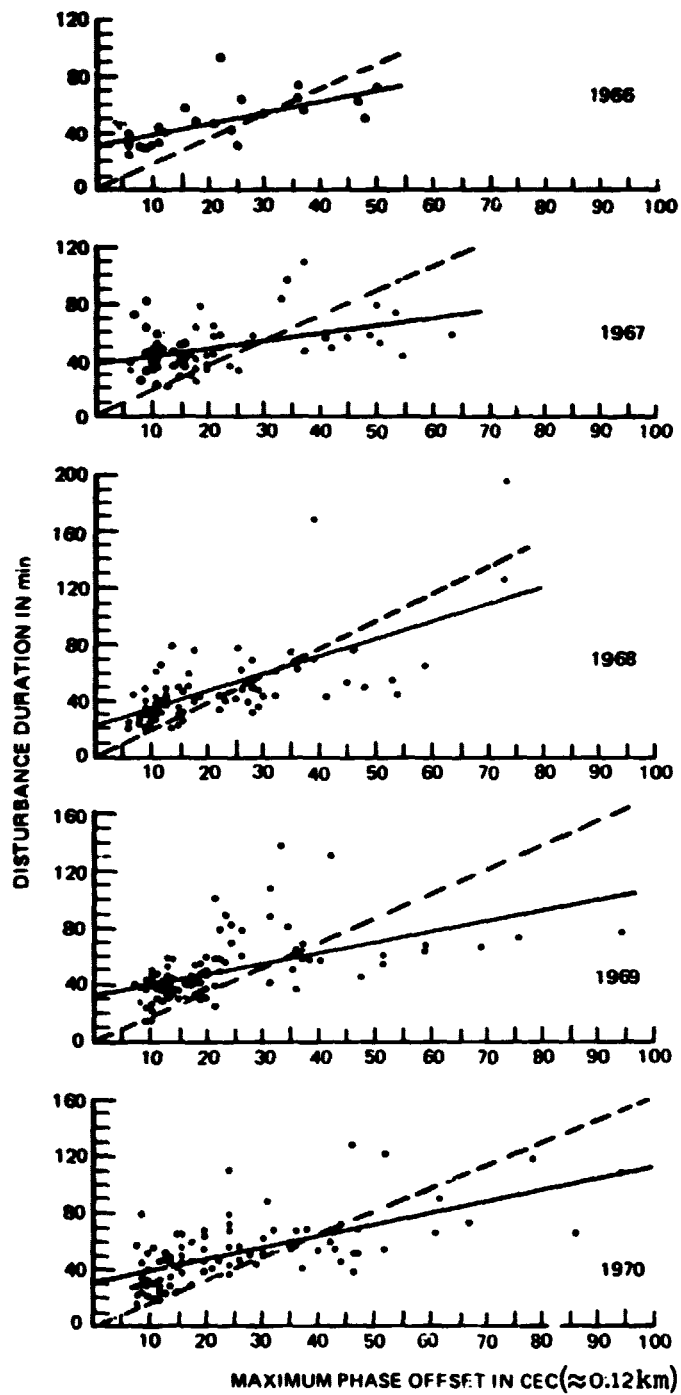


Figure 12. Disturbance Duration vs. Maximum Phase Offset for SPA Events on Hawaii to New York Path at 10.2 kHz

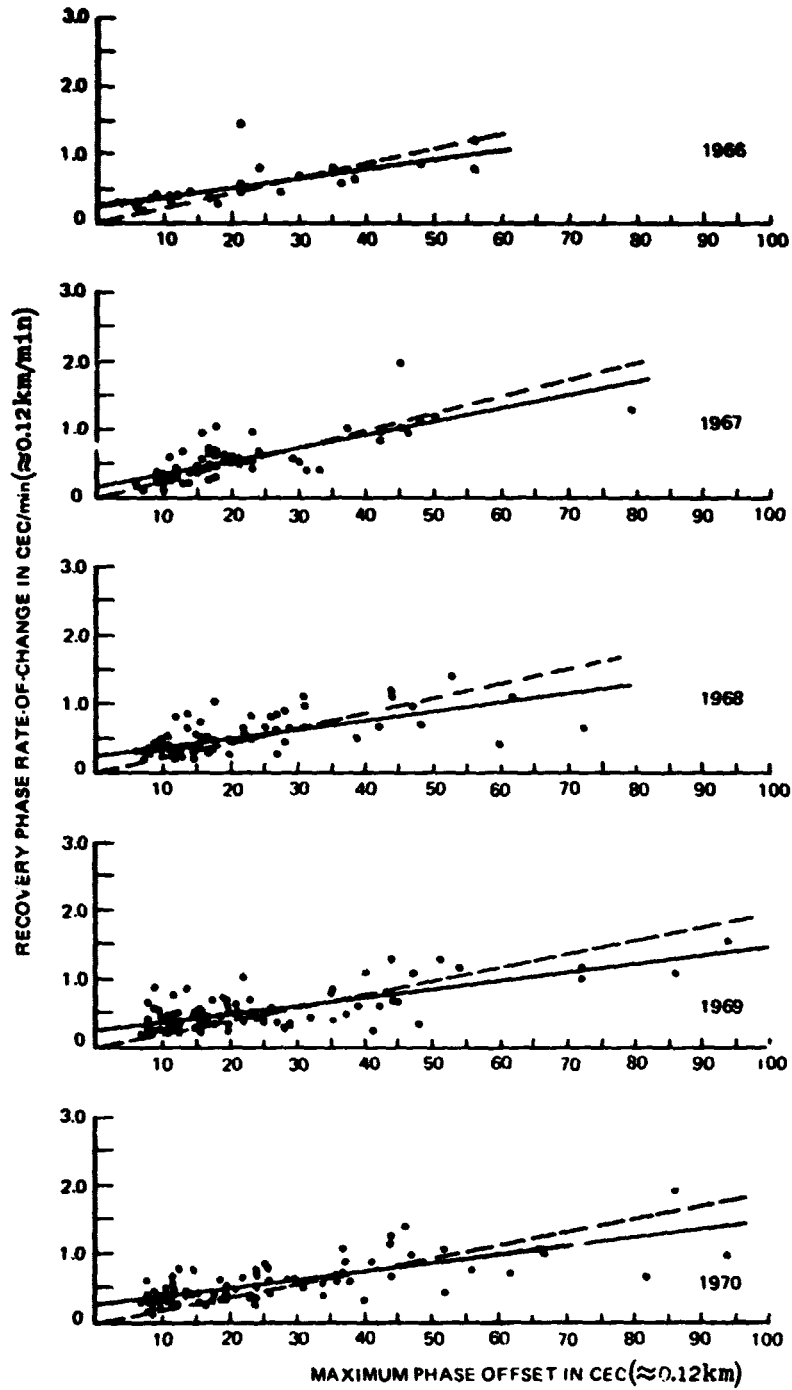


Figure 13. Recovery Phase Rate-or-Change vs. Maximum Phase Offset for SPA Events on Hawaii to New York Path at 10.2 kHz

Table II  
SPA Shape Correlation

YEAR	NO. OF SPAs	MAXIMUM PHASE OFFSET VS. ONSET RATE-OF-CHANGE $\Delta\phi_m \sim T_o \dot{\phi}_o$			TOTAL DURATION VS. MAXIMUM PHASE OFFSET $T \sim (1/\hat{\phi})\Delta\phi_m$			RECOVERY RATE-OF-CHANGE VS. MAXIMUM PHASE OFFSET $\dot{\phi}_R \sim (1/T_R)\Delta\phi_m$		
		$\hat{T}'_o$ (MIN.)	$\hat{T}_o$ (MIN)	$r_B$	$\hat{\phi}$ (CEC/MIN)	$\hat{\phi}$ (CEC/MIN)	$r_B$	$\hat{T}_R$ (MIN.)	$\hat{T}_R$ (MIN.)	$r_B$
1966	24	7.7	7.6	0.84	0.57	1.30	0.64	47.0	71.9	0.69
1967	68	6.7	5.4	0.56	0.57	1.95	0.42	40.8	51.3	0.79
1968	76	5.9	5.0	0.59	0.53	0.82	0.65	46.3	78.1	0.65
1969	99	5.4	3.2	0.38	0.58	1.33	0.53	51.6	82.0	0.72
1970	92	6.2	4.7	0.51	0.62	1.24	0.65	52.4	80.0	0.74

Notes: See Figure 2 for definition of terms. Primes indicate quantities determined by regression through origin (dashed lines in Figures 9-11). The quantity  $\hat{\phi}$  is the reciprocal of the estimated regression slope of T on  $\Delta\phi_m$  and similarly for  $\hat{\phi}$ ,  $\hat{T}_R$  and  $\hat{T}_R$ .

All correlation coefficients are significant in the statistical sense that the respective quantities are positively correlated at the 95% confidence level. However, no estimated correlation slope is sufficiently high to allow explanation of even half of the observed scatter, although about half of the statistical variance can be explained in estimating recovery time. Presumably, other unobserved geophysical variables such as the energy spectrum of the associated flares or ionospheric chemistry variations are significant in determining the interrelationships. This statistical explanation associated with the correlation slope is in addition to causal explanation in the sense that when an event is recognized, the mean future condition is expected. Specific relations are discussed in the following paragraphs.

Maximum phase offset as a function of onset phase rate-of-change is shown in Figure 11. Although the indicated correlations suggest slightly shorter onset durations in periods of higher sunspot activity, the yearly average onset durations so computed yield a standard deviation of only 0.8 cec about an overall average of 6.4 cec. The apparent quantization of rates is due to the measurement of onset slopes to the nearest degree.

Total duration as a function of the maximum phase offset is shown in Figure 12. The relationship is primarily causal; i. e., when an SPA has occurred, the duration will be typically about 45 minutes (see Fig. 5). There also is a tendency for larger SPA's to last longer. The median overall rate is 1.3 cec/min corresponding to 0.77 minutes per centicycle of observed phase perturbation, or equivalently, about 6 minutes duration per kilometer of effective ionospheric height change. There appears to be no significant difference between years of high and low solar activity.

Recovery phase rate-of-change is related to maximum phase offset in Figure 13. The indicated correlations are higher than for the two previous functional relationships and are sufficient to permit explanation of half of the variance in recovery rates in terms of maximum offset. The indicated recovery time is consistent with previous results (see Fig. 5) showing the range for typical-to-average total duration to be about 40-50 minutes. There appears to be no significant difference between years of high and low solar activity.

#### Spatial Variation: Normalization of SPA Magnitude for Solar Zenith Angle

Previous sections have discussed the statistical occurrence and distribution functions of SPA characteristics over a single path at one frequency and the interrelationship between SPA's at 10.2 and 13.6 kHz. Spatial effects on observed SPA magnitude will now be studied through the use of Rome, New York phase recordings of 10.2 kHz transmissions from both Hawaii and Trinidad. An initial scanning indicated that the onset times and durations of events observed near noon

were simultaneous to within the minute or so accuracy of the instrumentation and that the shapes were approximately similar. Detailed attention was then directed to the interrelationship between peak amplitudes and illumination conditions along the two paths.

Previous studies of diurnal phase variation at 10.2 kHz have shown that phase varies approximately proportionally to the normal component of solar flux near noon (although slightly modified by historical dependence).<sup>13</sup> Normal diurnal variation near noon is approximately as though the effective phase height were negatively proportional to the incident solar flux (cosine of the solar zenith angle) and the nominal phase velocity were varying negatively proportional to the phase height with no variation in the phase of the excitation factor associated with coupling-propagated energy into or from the earth-ionosphere waveguide. The foregoing arguments are consistent with experimental phase variation resulting from normal solar radiative flux variations producing ionization changes in the D-region near noon. We now ask whether these features are also appropriate for abnormal solar radiation such as produced by solar X-ray flares. The raw measurements were correlated to obtain the assumed linear proportionality between maximum phase offsets on the two paths:  $\Delta\phi$  Trinidad - New York = 0.44 ( $\Delta\phi$ ) Hawaii - New York = 0.2 cec. The raw measurements also were normalized by division by the respective path average cosines of the solar zenith angles and essentially the same result was obtained from the correlation both numerically and in quality of fit. Apparently the zenith angle criterion is a poor method of normalization. A further comparison was made by correlating measurements where the average solar zenith angle over both paths was much the same so as to reduce complexity by minimizing differences in path illumination conditions. In this case, a coupling proportionality constant of 0.39 was obtained compared with 0.44 obtained earlier.

The constant of proportionality between the magnitude of SPA's observed over the Hawaii - New York path and those observed on the Trinidad - New York path may be estimated theoretically. For the two paths in question secondary velocity variations, such as with path azimuth, are not expected to be large nor is the excitation factor expected to vary significantly for illumination near noon.<sup>14</sup> Thus the coupling constant should be proportional to effective path length ratio. The actual total path length ratio is  $0.49 = (3843 \text{ km} / 7814 \text{ km})$  but propagation theory developed for the Omega signals<sup>15</sup> recognizes a region of excitation or de-coupling from the earth-ionosphere wave guide of 680 km ( $6.1^\circ$  of arc on the earth's surface) at each end. Thus the effective path length is  $2 \times 680 \text{ km}$  shorter than the geometric path length and the effective path length ratio for the two paths studied is  $(3843 - 1360 \text{ km} / 7814 - 1360 \text{ km}) = 0.39$ , which was the experimental ratio obtained when data were selected so as to minimize differences in illumination conditions. Thus the experimental results are consistent with present theory on the spatial aspects of VLF propagation including the effective path length

concept but are not consistent with zenith angle normalization. A possible explanation may be that the phase received is not linearly related to the normal component of X-ray flux over a path due either to ionization equations governing the relationship between effective phase height and input energy or a non-linearity between effective phase height and velocity. In practice both may be present to some degree. Certainly, theory indicates marked non-linearity in the relationship between phase height and velocity for heights between 60 and 70 km, the range needed for the larger SPA's. Non-linearity between ionospheric phase height and input flux is also believed likely. Although beyond the present scope of effect, it would appear possible to deduce the relationship between ionospheric phase height and high level solar flux input through further analysis of SPA's. Further analysis using the methods suggested here together with the more elaborate methods of Reference 4 appears particularly inviting.

#### CONCLUSIONS

The foregoing synoptic study of 500 SPA's observed between 1961 and 1970 in New York yields the following description of a typical SPA. A rather abrupt phase variation occurs reaching a maximum offset in about 6 minutes with the total duration of the event being about 45 minutes. Typical maximum offsets are about 15 cec at 10.2 kHz on the Hawaii - New York path corresponding to 15 microseconds or ionospheric phase height changes of 1.8 km. Typical observed phase rates of change during onset were 3.5 cec/minute corresponding to frequency shift of  $6 \times 10^{-8}$  or a rate-of-change of ionospheric phase height of 0.4 km/minute; recovery rates of change are 0.5 cec/minute corresponding to a frequency variation of  $4 \times 10^{-9}$  and ionospheric height change rate of 0.06 km/minute. SPA's are observed simultaneously over the different paths and at the two different frequencies investigated. The occurrence of SPA's is related to sunspot activity with about one per day being observed somewhere on earth when the sunspot number is about 85. The probability of a SPA occurring nearly vanishes during very low sunspot activity. Although sufficiently rare that SPA-associated phase variations exceed nominal propagationally-induced phase scatter only about 5% of the time even during high sunspot activity, SPA's are of practical as well as geophysical and astrophysical interest. VLF navigation, timing, and communications systems are expected to work safely, accurately, and reliably most of the time. It is primarily during unusual conditions that additional attention is needed to avoid false readings during these anomalies.

## REFERENCES

1. Solar Flares and Space Research, Edited by C. DeJager and Z. Svestka, North-Holland Pub. Co., Amsterdam 1969 (Prod. of Committee on Space Research Symposium, Tokyo, 9-11 May 1968).
2. Reder, F. H., "VLF Propagation Phenomena Observed During Low and High Solar Activity", (paper presented 19 Aug 1969 at XVI General Assembly of URSI, Ottawa, Canada).
3. Reder, F. H., and S. Westerlund, "VLF Signal Phase Instabilities Produced by the Propagation Medium: Experimental Results," (AGARD Conference Proc. as for 10 below.
4. Naval Electronics Laboratory Center Technical Report 1868, A D-Region Model which Accounts for Quiet and Disturbed VLF Propagation Phenomena by M. P. Bleiweiss, V. E. Hildebrand, and J. R. Hill, 30 March 1973.
5. Swanson, E. R., "Omega", Navigation, V. 18, No. 2, pp. 168-175, Summer 1971.
6. Swanson, E. R. and Kugel, C. P., "VLF Timing: Conventional and Modern Techniques Including Omega", Proceedings IEEE 60, No. 5 pp. 540-551, May 1972.
7. Naval Electronics Laboratory Center Technical Report 1740 (Rev.), Omega VLF Timing, by E. R. Swanson and C. P. Kugel, 29 June 1972. AD743529.
8. Naval Electronics Laboratory Center Technical Document (in preparation), Omega VLF Phase Difference Data Series, Volume 1, Rome, N. Y.
9. Naval Electronics Laboratory Center Technical Report 1757, Omega Synchronization and Control, by E. R. Swanson and C. P. Kugel, 19 March 1971. AD732448.
10. Swanson, E. R., "Time Dissemination Effects Caused by Instabilities of the Medium", North Atlantic Treaty Organization Advisory Group for Aerospace Research and Development, Electromagnetic Wave Propagation Committee, Phase and Frequency Instabilities in Electromagnetic Wave Propagation, Editor K. Davies, Slough England Technivision Services, 1970 (AGARD Conference Proceedings No.33), pp. 181-198.

11. Crombie, D. D., "Phase and Time Variations in VLF Propagation Over Long Distances", *Radio Science, Journal of Research, NBS*, Vol. 68D, No. 11, p. 1223, November 1964.
12. "ESSA Research Laboratories, "Daily Solar Indices," Solar Geophysical Data, Part I, 1960-1970.
13. Naval Electronics Laboratory Center Technical Report 1781, Diurnal Phase Variation at 10.2 kHz, by E. R. Swanson and W. R. Bradford, 11 August 1971. Ad737212.
14. Swanson, E. R., "VLF Phase Prediction", VLF-Propagation: Proceedings from the VLF Symposium, Sandefjord, Norway, 27-29 October 1971, G. Bjøntegaard, Ed., pp. 8-1 to 8-36, (Norwegian Institute of Cosmic Physics Report 7201, January 1972)

## QUESTION AND ANSWER PERIOD

### QUESTION:

I see the great correlation with sunspot activity in many other fields of science, but I see a weak point, and ask you what significant data do you have of any activity that takes place on the other side of the Sun?

### MR. SWANSON:

The solar forecasters do take into account and often will, say, call for a higher probability of activity, say, 12 or 13 days after activity was last observed on the ground — the spot group then reappearing on the other limb.

For the type of use that I have made of it here, I don't know if it is all that fair to tie it to a sunspot number directly, or whether it should be into the phase of a basically 11 year solar phenomenon. I wouldn't argue that.

Really, in the short run, it is clear that if you know the types and spots and whether or not they are there, or whether the evolution of spots on the Sun in the past few weeks has gotten them to be there, you can be far more deterministic about it. These reports are issued regularly, incidentally, both by Boulder and by the Cheyenne mountain forecast. It is still, I am afraid, somewhat of a black art, but it is getting more refined.

### DR. WINKLER:

It appears to me that for practical application, time service, for instance, the probability measure is of relatively little importance. All you can say is next week it is going to be bad, and you will probably have a number of disturbances, but you will still be unable to say when they will come and how large they will be.

What is your opinion about comparing or correlating the various frequency difference, or phase differences, with the view toward telling the operator at the moment that he has a disturbance of so many microseconds? That is really going back to Pierce's composite phase technique.

### MR. SWANSON:

The correlations there are high, but not entirely perfect. I think it is worth a try. Let's face it, this is what we do. We shouldn't lose sight of this, it is an accepted technique and has been for years. If you want to adjust a frequency standard or something of that sort, you start making a phase track as a function of your local clock, and you do this more or less in the daytime. If there is a

sudden phase anomaly, the track makes an obvious runoff, and you say, oh, there was a Sudden Phase Anomaly. You wait for an hour and it goes away, and you are back to measuring again.

This is perfectly valid. Really that technique has basically the navigational counterpart which is to get a good dead reckoning of where you are going. We know from these distributions that when the event occurs the runoff would be fairly rapid. Your integration time is most likely on the order of a minute anyway.

So, we are talking here of only a couple of integration times before we are beginning to get a good estimate that there has been an event. This is a very realistic environment.

So, both the auto-correlated property, or sudden failure of it, is a good indication of an SPA as well as the inner comparison in the event at several frequencies. I think most of the time we avoid these because they are so obvious. The danger is mostly if you are using an automatic system or something of that type.

DR. REDER:

We had made some studies of finding out whether we can predict or whether we can say from a measurement, let's say on NPM at 23.4 kilohertz, whether we can say—at Fort Monmouth—what it would be on 10.2, Haiku, Hawaii, which is the same path.

And we are very happy because everything seemed to work out very fine. Unfortunately, I made some mistakes, and when I applied it to Trinidad at Fort Monmouth, it didn't work at all.

MR. SWANSON:

We did check the simultaneity of events on the Haiku to Rome, and also Trinidad to Rome path.

DR. REDER:

No, I am not talking about the simultaneity. This works fine. The problem was can it predict the size of the maximum phase, and this is the problem.

MR. SWANSON:

That very subject is in the paper. I didn't go into it here, partly because of the complexity. It is not as easy as you might think. It does not go strictly in a linear way with zenith angle, as the normal diurnal change would, near noon. Nor does it go strictly with the path length, apparently.

Well, one would think the process perhaps is more easily explained than it is. I think there are some reasons that it doesn't work quite the way you would like it to.

DR. REDER:

Yes, but Eric, the problem is it doesn't even work always on the same path, at the same time. That is the problem.

In other words, NPM to some location and Haiku to some location. We have three frequencies, 10.2, 13.6, and 11-1/3 kHz. Sometimes it will work very well using some kind of ionospheric model, and then comes an SID and it doesn't work at all.

Apparently, it means that it has a lot to do with the spectrum of the solar atmosphere, and that we have to take it into account.

MR. SWANSON:

I am sure this is an element. I think it is probably also true that over any of these long paths there is quite an array of the solar zenith angles, and I think, as you get more of a flare flux, the depression of the ionosphere, if you will, and the phase response to this depression, both will become non-linear.

So, now you say, I want a zenith angle, and what are we talking about. If we are talking about the average, we know that is wrong all of a sudden. It is a non-linear effect here. I have my own speculative feelings that one might be able to pull inversions, and deduce the relationship in essence between say velocity or effective phase height and the zenith angle, the flux component, by running studies of this sort.

In this regard, there is also the alternative approach of going directly to the aeronomy models using flux input on a particular flare, such as are available from the Solarad system.

**DR. REDER:**

**Eric, it is a great pleasure to notice that whenever you don't know an answer you rely on non-linearity. Welcome to the club.**

**MR. SWANSON:**

**I am giving two approaches. I don't know how the non-linear lies, but I do know there are two. If you take even a simplistic model such as Wait published years ago, and look at the partial of the velocity with respect to the nominal height, as the ionospheric height levels go down toward 60 kilometers, it becomes a much wider spread in velocity than is true about, say, near 80. 70 to 80 is maybe half the velocity change than 60 to 70 is.**

**I think that the other half of the coin is what happens to the aeronomy given the flux coming in, and I suspect that is non-linear also.**

**MR. EASTON:**

**Thank you very much, Eric.**

C-6